GENERAL ATOMIC

CONF-770807--6

GA-A14329

RESIDUAL STRESSES IN PEACH BOTTOM TEST ELEMENTS
ANALYSIS vs. EXPERIMENT

by

W. G. Homeyer, F. K. Tzung, and D. D. Chiang

March 1977

DISCLAIMER

GENERAL ATOMIC

GA-A14329

RESIDUAL STRESSES IN PEACH BOTTOM TEST ELEMENTS
ANALYSIS vs. EXPERIMENT

by

W. G. Homeyer, F. K. Tzung, and D. D. Chiang

This is a preprint of a paper to be presented at the 4th International Conference on Structural Mechanics in Reactor Technology, August 15-19, 1977, San Francisco, California.

Work supported by the U.S. Energy Research and Development Administration, Contract EY-76-C-03-0167, Project Agreement No. 17.

General Atomic Project 3224 March 1977

TABLE OF CONTENTS

LIST OF FIGURES

LIST OF TABLES

1. SUMMARY

Operating stresses and residual shutdown stresses in fuel test elements irradiated in the Peach Bottom Reactor were calculated with finite element methods. Calculations of deformation and stress due to primary loads were also made. Results of the calculations were used to develop an experimental analysis of graphite fuel and reflector elements. Measured deflections and fracture loads were then compared with predictions made with the analytical methods and data to be verified.

Thirteen graphite bodies from eight test elements were analyzed. All of these were in the form of hollow cylinders 70 mm in diameter by 8.3 mm long which had six or eight fuel holes evenly spaced around the cylinder. The various bodies were irradiated to fast neutron fluences ($E > 0.1$ Mev) between 0.3 and 4.0×10^{25} n/m^2 at temperatures between 850 and 1650°K.

Residual axial stresses in the elements were calculated to reach 15.7 MPa compared to a strength of 22.8 MPa while in-plane stresses were calculated to reach 15.8 MPa compared to a strength of 11.5 MPa. For the eight-hole teledial elements, peak in-plane stresses were found to be at a sharp notch, where the stress calculations were believed to be unreliable. In-plane stresses at other locations, where the stress predictions were expected to be more reliable, reached 11 MPa.

A number of experiments were designed as a result of the calculations. Portions of the fuel bodies were cut into longitudinal strips of 460 mm length. The expected bow of the strips due to the gradient in residual axial stress was calculated to range between 0.5 and 3 mm by applying elastic beam theory to the results of the residual stress calculation. The measured bow was less than half of that calculated or was reversed in direction. The reversals occurred in some of the strips exposed to conditions of higher fluence and temperature. Further experiments are in progress to determine if the discrepancies are due to microstructural changes caused by the saw blades during the cutting operation.

Experiments to study residual in-plane stresses were designed to used 2-cm-thick ring-shaped disks cut from the test elements. Some of the disks were slit through one side along a plane through the axis of the element, and the extent of closure of the ring due to the relief of the gradient in in-plane (hoop) stress was measured. The calculated deformations of 0.15 to 0.3 mm were in reasonable agreement with the measured deformations.

Some of the disks were loaded to failure by compression between two plates, while others were tested by pressurizing fuel holes to failure. Unirradiated disks were also tested, and the failure loads were compared. The irradiated disks were found to be stronger in cases where the residual stresses at the point of failure were compressive or zero, but weaker where there were large residual tensile stresses at the point of failure. Both observations were consistent with predictions. The tests of unirradiated specimens also showed that failure stresses exceeded the uniaxial tensile strength by factors of 1.5 to 4.3 due to the nonuniform stress in the specimens.

The program of methods verification has shown there is good agreement between analysis and experiment in some cases but large discrepancies in others. Where there are discrepancies, they generally indicate that the methods are overestimating the magnitude of the residual stresses.

2. INTRODUCTION

A number of 6-hole and 8-hole teledial test elements were irradiated in the Peach Bottom High Temperature Gas Cooled Reactor (HTGR) to various levels of temperature and fast neutron fluence. Although the elements were irradiated for the primary purpose of testing fuel particles and rods, these test elements were found to provide an excellent source of irradiated graphite bodies for use in verifying the structural design methods used for HTGR fuel elements.

The fuel test elements were analyzed to predict the residual stresses in the graphite bodies after irradiation. These residual stresses, or end-of-life shutdown stresses, tend to be at or near the highest stress reached in the fuel body during irradiation. They result from the combined effects of irradiation-induced shrinkage and thermal shrinkage on cooling to room temperature from operating conditions with operating temperature gradients.

The residual stress distribution was used at first to design a test program to measure the effects that the residual stresses would have on deformation and on failure loads. Calculations of stress distribution due to primary loads were also made to help in defining tests. Tests included cutting of longitudinal strips and rings, radial compression of discs, and pressurization of fuel holes. As preliminary results of the test program became available (Wallroth, et. al.[1]), the predictions of deformation and failure load based on the stress calculations were compared directly with the experimental results.

3. STRESS ANALYSIS

The GTEPC computer code, a two-dimensional finite element program (Tzung[2]), was used for temperature and stress computations. A standard solid model (Head[3]) was adopted to account for the irradiation-induced creep in graphite. Material properties were varied with fast neutron fluence and temperature of irradiation according to the data of Beavan[4].

The residual stress depends on the thermal and irradiation history. The thermal boundary conditions, heat generation rates, and fast neutron flux at various times during irradiation in the Peach Bottom reactor were developed as described, e.g., by Wallroth, et. al.[5]

3.1 Residual Stresses

The finite element models used for thermal calculations are shown in Figures 1 and 2. They are symmetrical sectors of the element with angles of 0.393 rad (22.5°) for 8-hole bodies and 0.524 rad (30°) for 6-hole bodies. For stress calculations, only the graphite portion of the models shown in Figures 1 and 2 were used. The operating and the shutdown stress fields resulting from the temperature differences and the neutron dose were computed on the assumption of generalized plane strain with no externally applied forces. Since axial temperature and strain gradients are much less than the in-plane gradients, the generalized plane strain assumption is expected to provide an adequate representation of the stress state except near the top and bottom ends of the graphite bodies.

The calculated residual stress distribution in the axial direction for typical 8- and 6-hole teledial elements are shown in Figures 3 and 4. This stress distribution, with tension near the center of the element and compression near the outside diameter, is caused by thermal and irradiation shrinkage. The central portion of the element shrinks more rapidly under irradiation because irradiation strain rates are higher at the higher

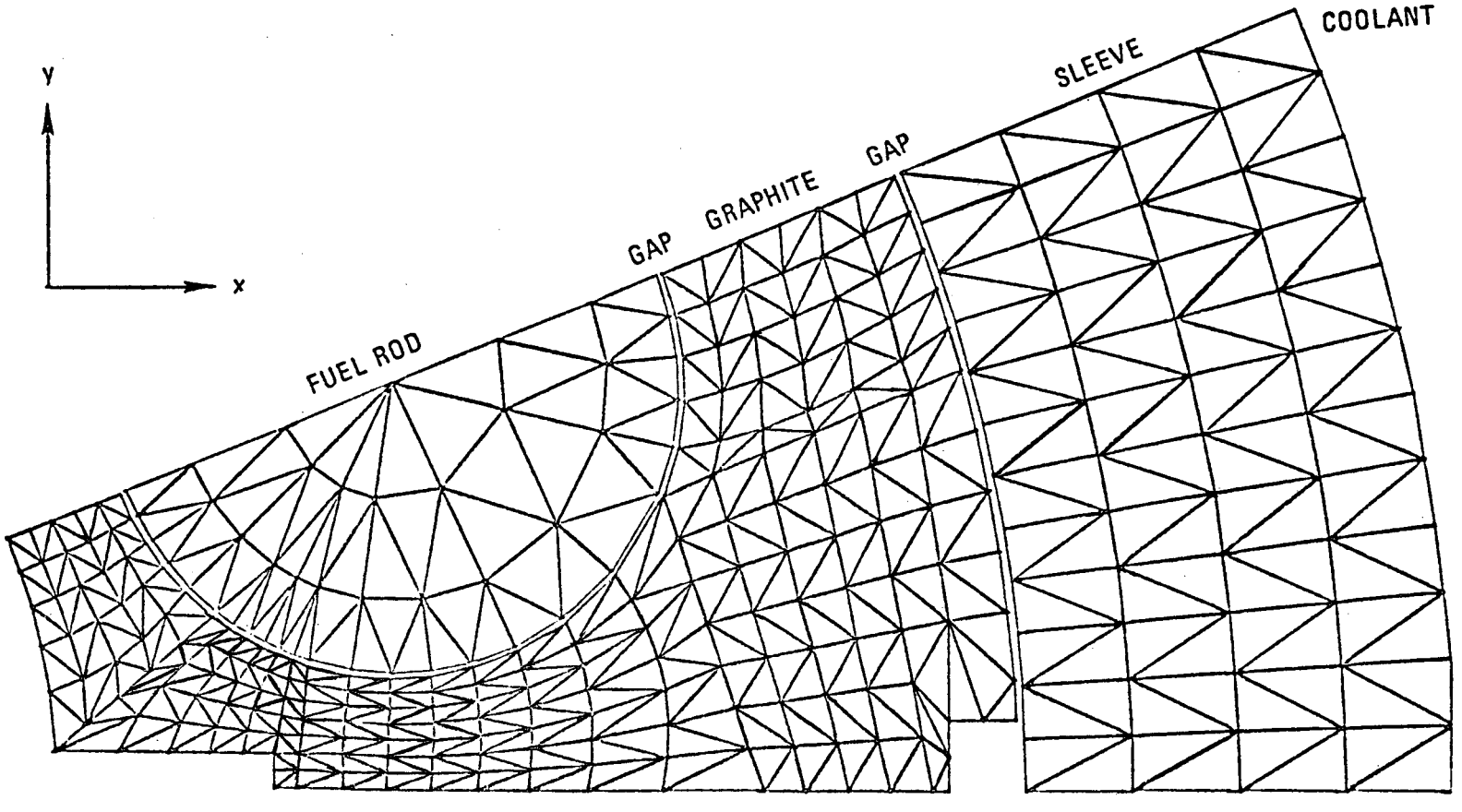

Figure 1 Finite element model for thermal analysis of 8-hole element.

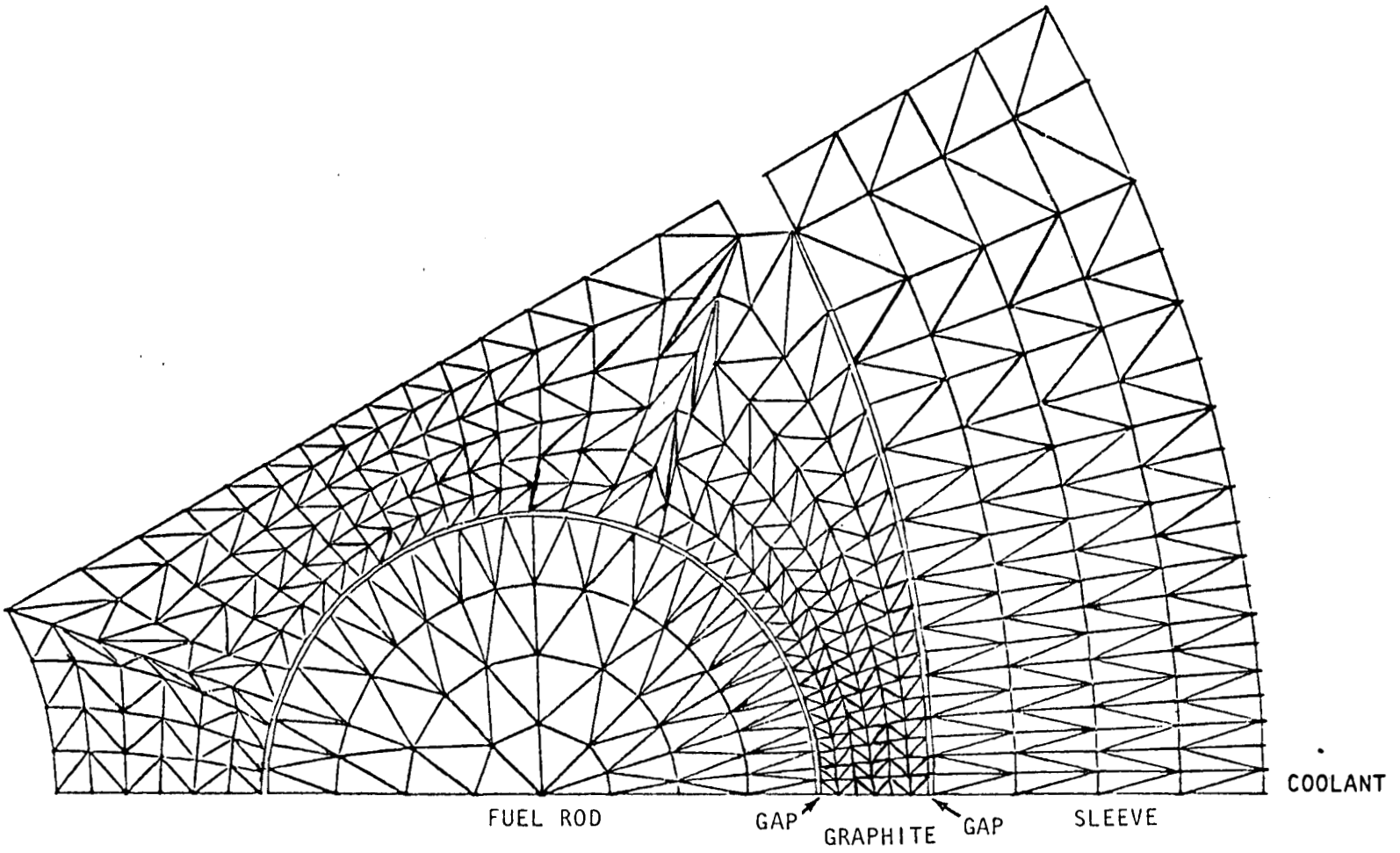

Figure 2 Finite element model for thermal analysis of 6-hole element.

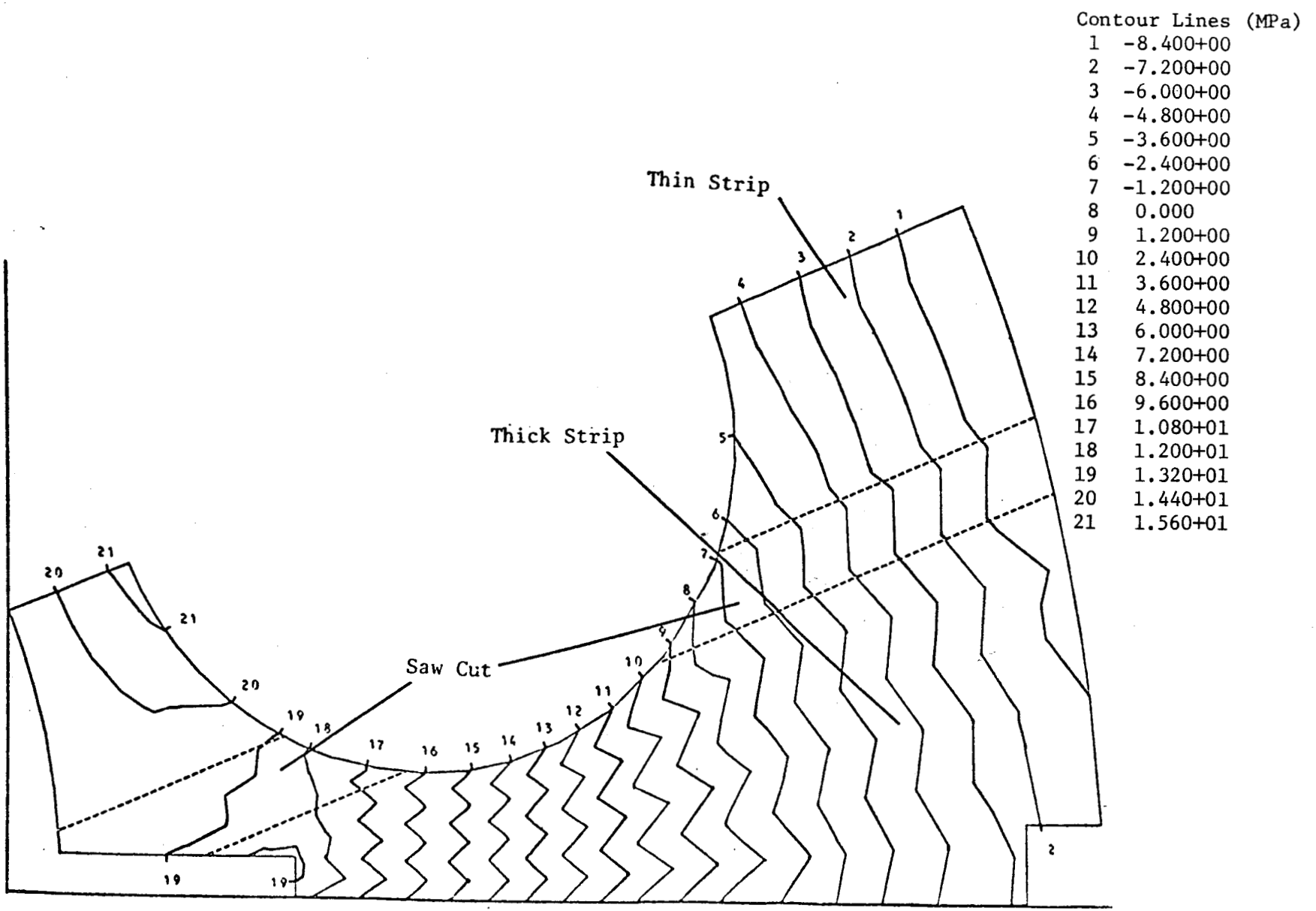

Figure 3 Residual axial stress for 8-hole element.

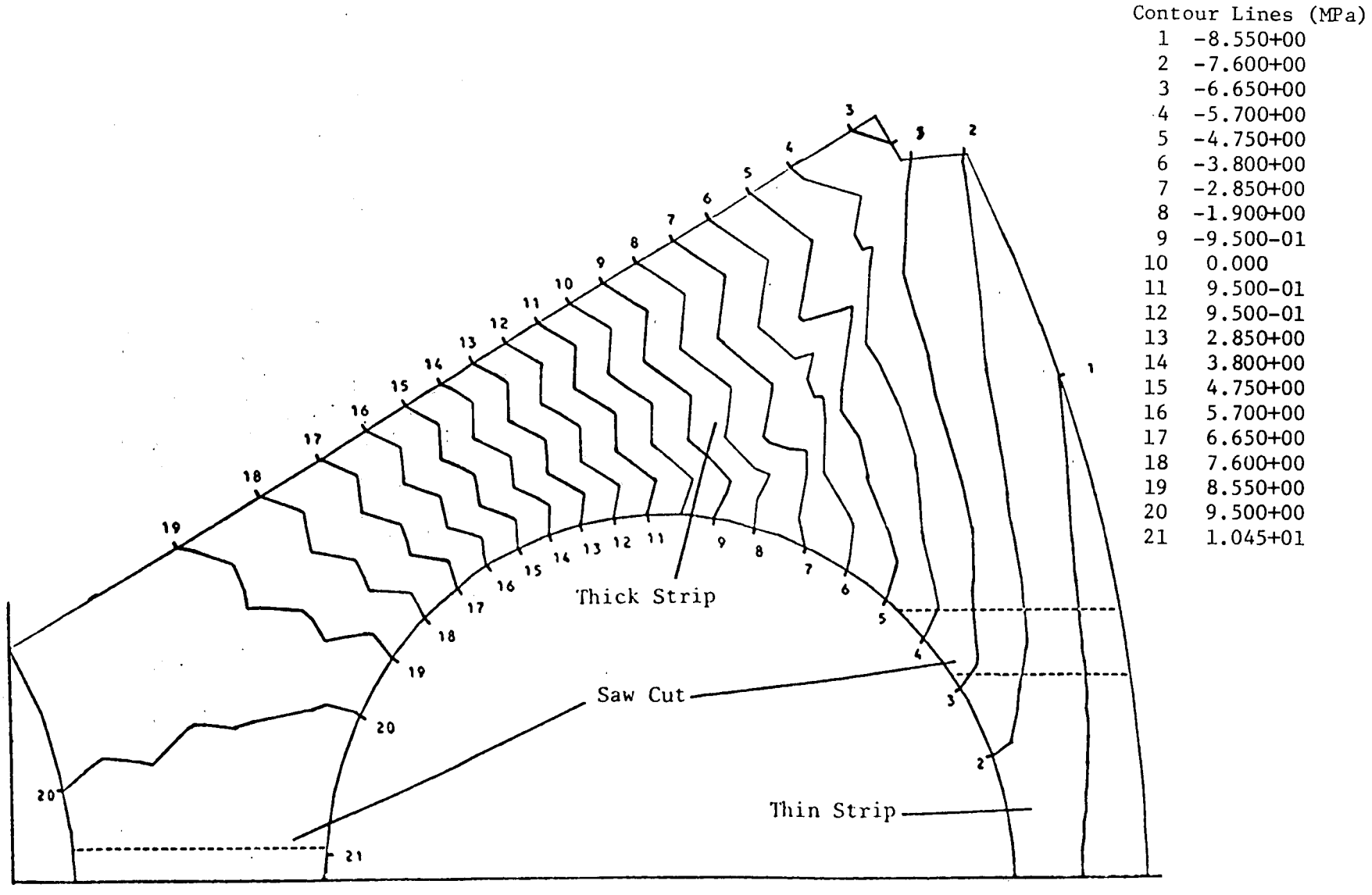

Figure 4 Residual axial stress for 6-hole element.

temperature in the center. When the reactor is shut down, the hotter central portion also contracts more thermally on cooling to room temperature. As a result, the residual stresses in the test elements are at or near the peak stresses reached during irradiation.

The relatively linear axial stress distributions in Figures 3 and 4 (note the herring-bone pattern is merely an artifact of the finite element mesh) suggested that strips be cut as shown. The relative length change of each strip was predicted from the average stress over the cross-section of the strip while the radius of curvature of bow was predicted from the stress distribution in the strip by applying beam theory. A length of 0.45 m was selected to give specimens short enough to be cut and handled but long enough for the bow and length change after cutting to be measureable. This length also leaves enough material from each of the 0.8-m-long test element bodies for in-plane stress investigations.

Typical calculated residual in-plane stress distributions are shown in Figures 5 and 6, in which maximum principal in-plane stress contours are plotted. The peak in-plane tensile stress (Figure 5) in the 8-hole elements is predicted to occur next to the slot cut into the inside of the element. (The slot was originally cut to assure that any breakage of graphite due to swelling of experimental fuel rods would be confined to the inside diameter of the element.) Stresses at the slot were shown to be sensitive to the finite element model; i.e., the peak stress was increased by 65% when a finer mesh was used. It appears that other effects, such as the non-linearity in the stress-strain curve of graphite, must be considered to predict stresses at the slot accurately. As shown in Figure 5, the stress is also high at the surface of the fuel hole nearest the center of the element. The peak in-plane tension in the 6-hole element (Figure 6) is a bending stress at the fuel hole surface caused by compressive stress in the thin, curved web between the fuel hole and the outer surface of the element.

The calculated in-plane stress distribution in both types of elements, with hoop tension near the inner surface and hoop compression near the outer surface, suggested experiments to verify the stress distribution. Discs 20 mm

Figure 5 Maximum principal in-plane residual stress for 8-hole element.

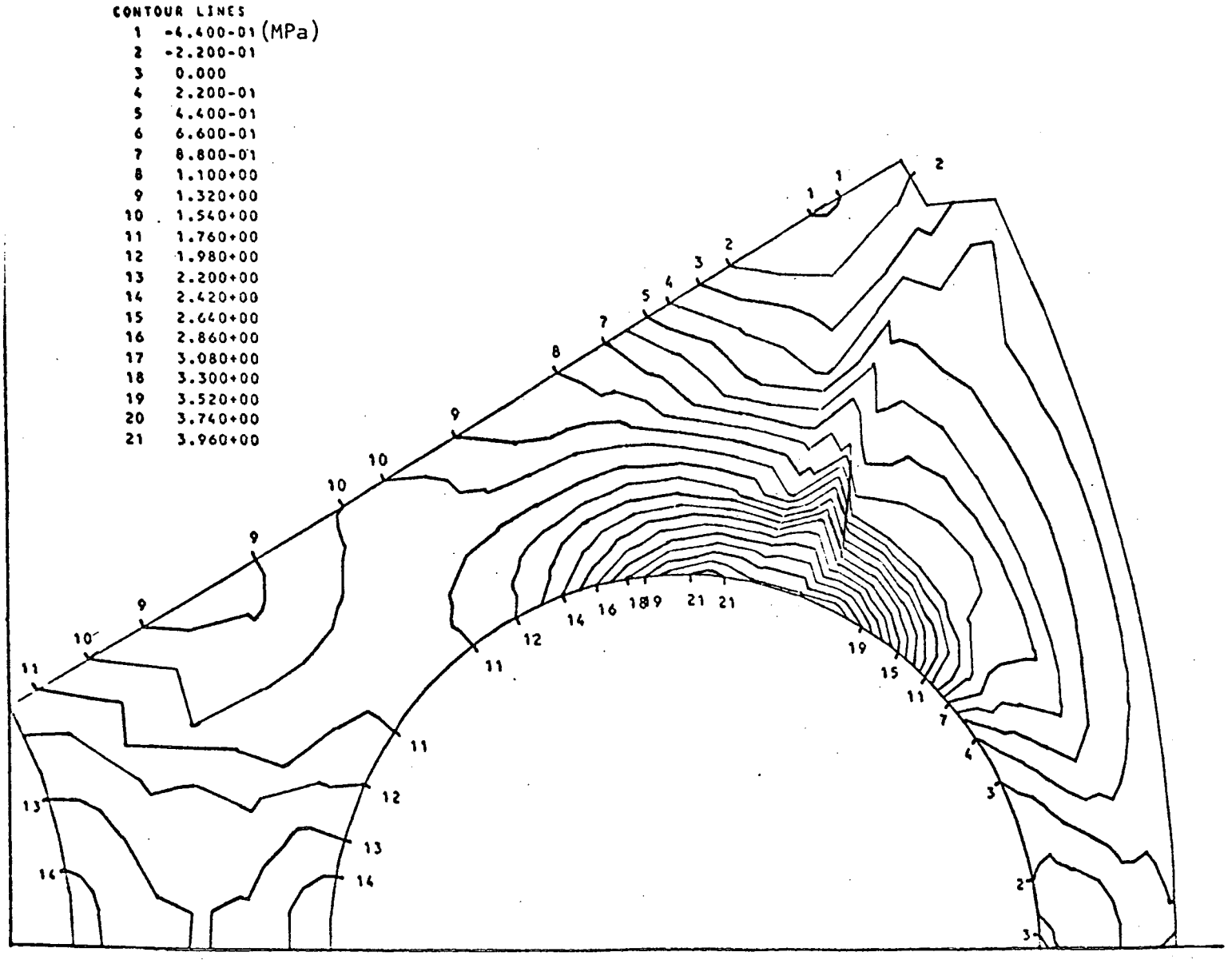

Figure 6 Maximum principal in-plane residual stress for 6-hole element.

thick cut from graphite test element bodies are used as specimens. The diameter and distance between grooves are measured as shown in Figure 7 before and after a cut is made through one side of the ring. The diameter and groove distance are predicted to decrease after cutting due to the release of the in-plane bending moment and a reduction in the radius of curvature of the ring.

3.2 Stresses Due to Primary Loads

Stresses due to primary loads were calculated using 1.57 rad (90°F) sector models such as that shown in Figure 8 for the 8-hole element. The maximum in-plane stresses due to pressurization of a fuel hole are shown in Figures 9 and 10 for 8- and 6-hole elements. Figure 9 shows that the peaks in in-plane tension from pressurization occur at the same locations as the residual stress peaks (Figure 5). This indicates that residual stresses will reduce the burst pressure for 8-hole teledial elements. The peak tensile stresses in Figure 10 are on the outside diameter near the fuel hole in a region where the residual stress is in compression. This indicates that residual stresses will not reduce the burst pressure for 6-hole teledial elements.

The calculated maximum principal in-plane stresses due to radial compression loads are shown in Figures 11 and 12 for the 8- and 6-hole elements. For 8-hole elements (Figure 11) peak tensile stresses are at the same 2 points as peak residual stresses (Figure 5), indicating that the residual stresses will decrease failure loads. For 6-hole elements (Figure 12) the peak tensile stress is in a region where the residual stress is compressive.

As a result of the primary load analysis, both radial compression and pressure burst tests on 20-mm-thick disc specimens were planned. It was also planned to measure load-deflection curves to compare with the predicted elastic modulus of the irradiated element. (Note: 4-point bend tests including load-deflection curves were planned for strips to measure the irradiated elastic modulus in the axial direction.) Radial compression tests were also planned to be performed on sections with 4 webs (designated a and b in Figure 11) removed by prior pressure-burst tests. The purpose

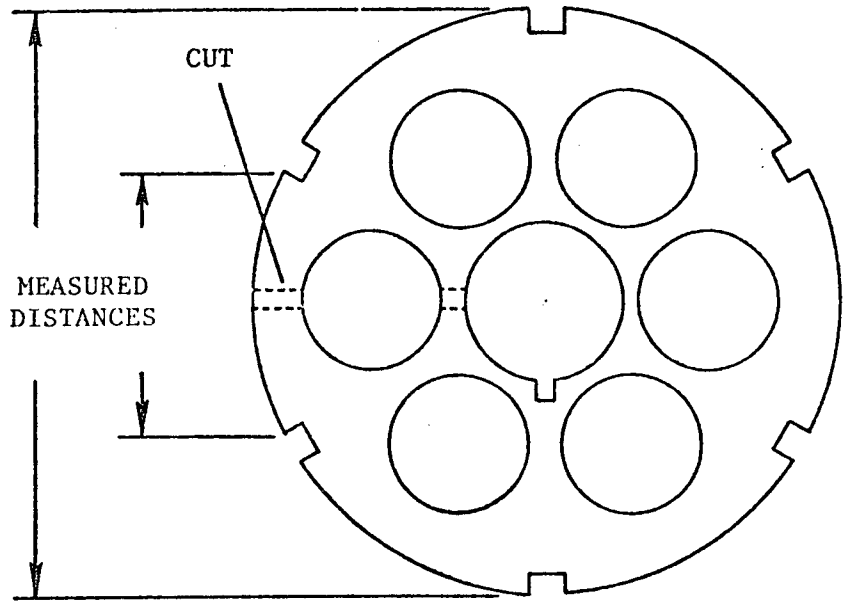

Figure 7 Specimen for ring-cutting tests.

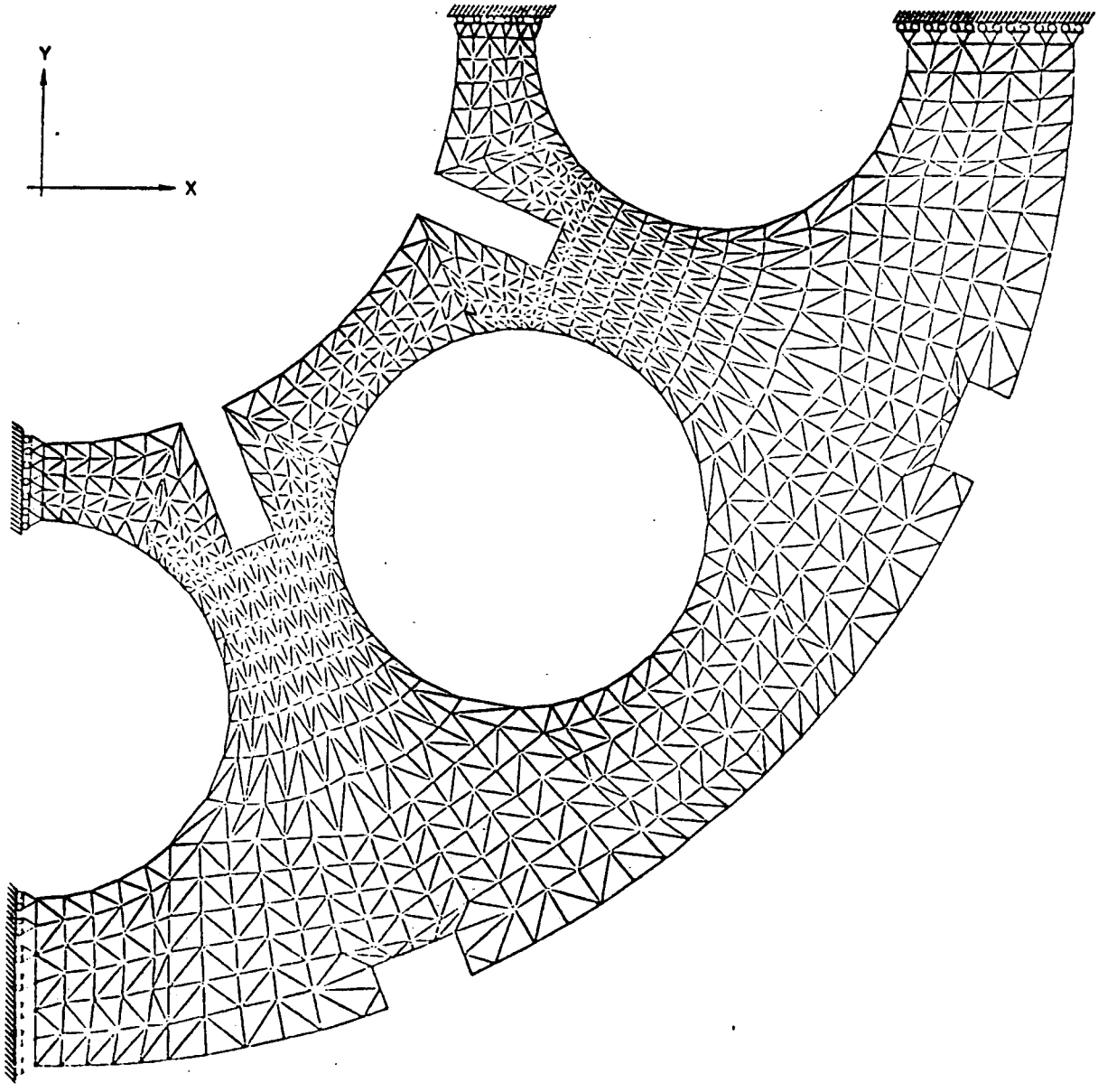

Figure 8 Finite element model for primary loading analysis.

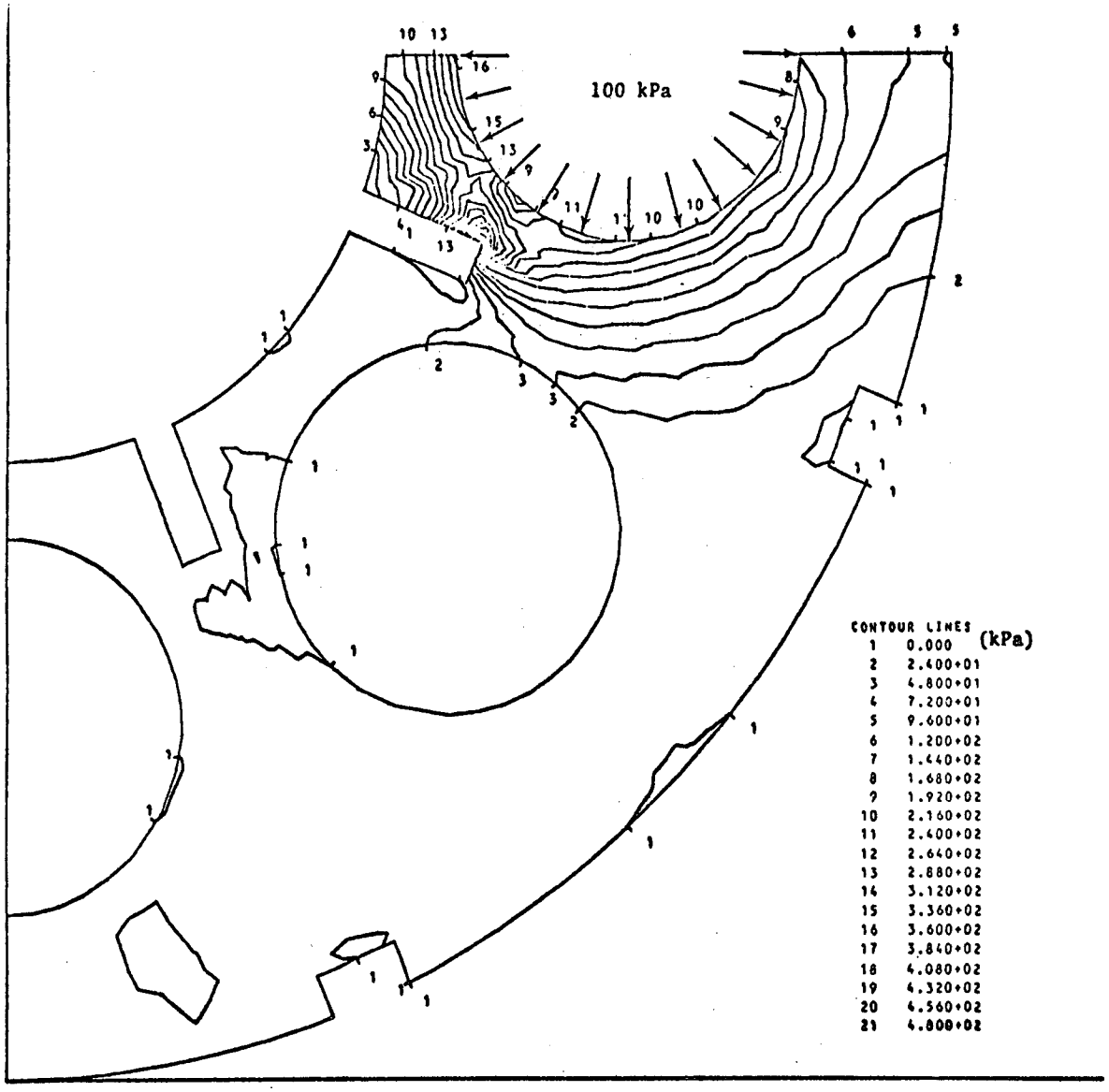

Figure 9 Maximum principal stress in 8-hole specimen under 100 kPa pressure load.

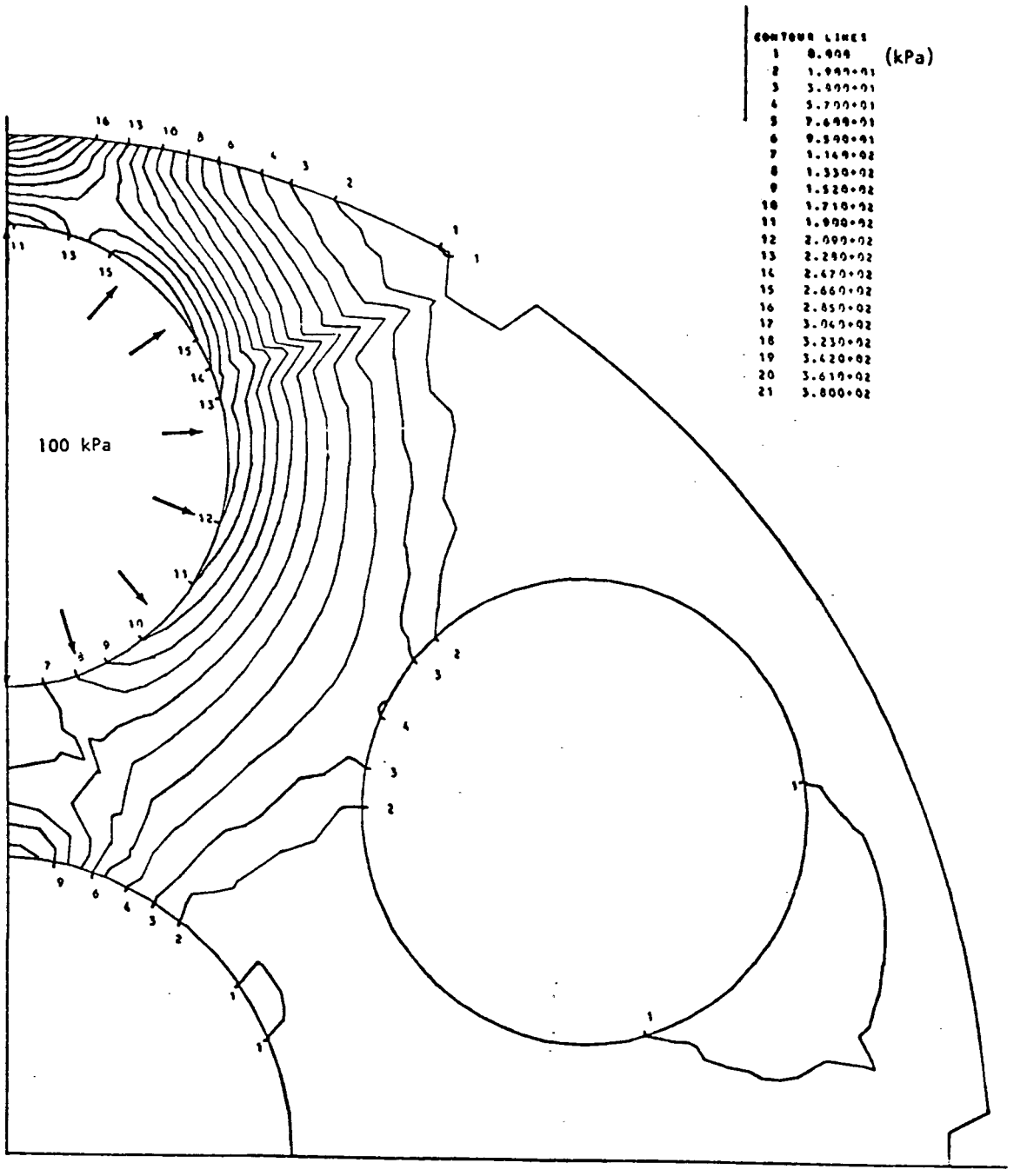

Figure 10 Maximum principal stress in 6-hole specimen under 100 kPa pressure load.

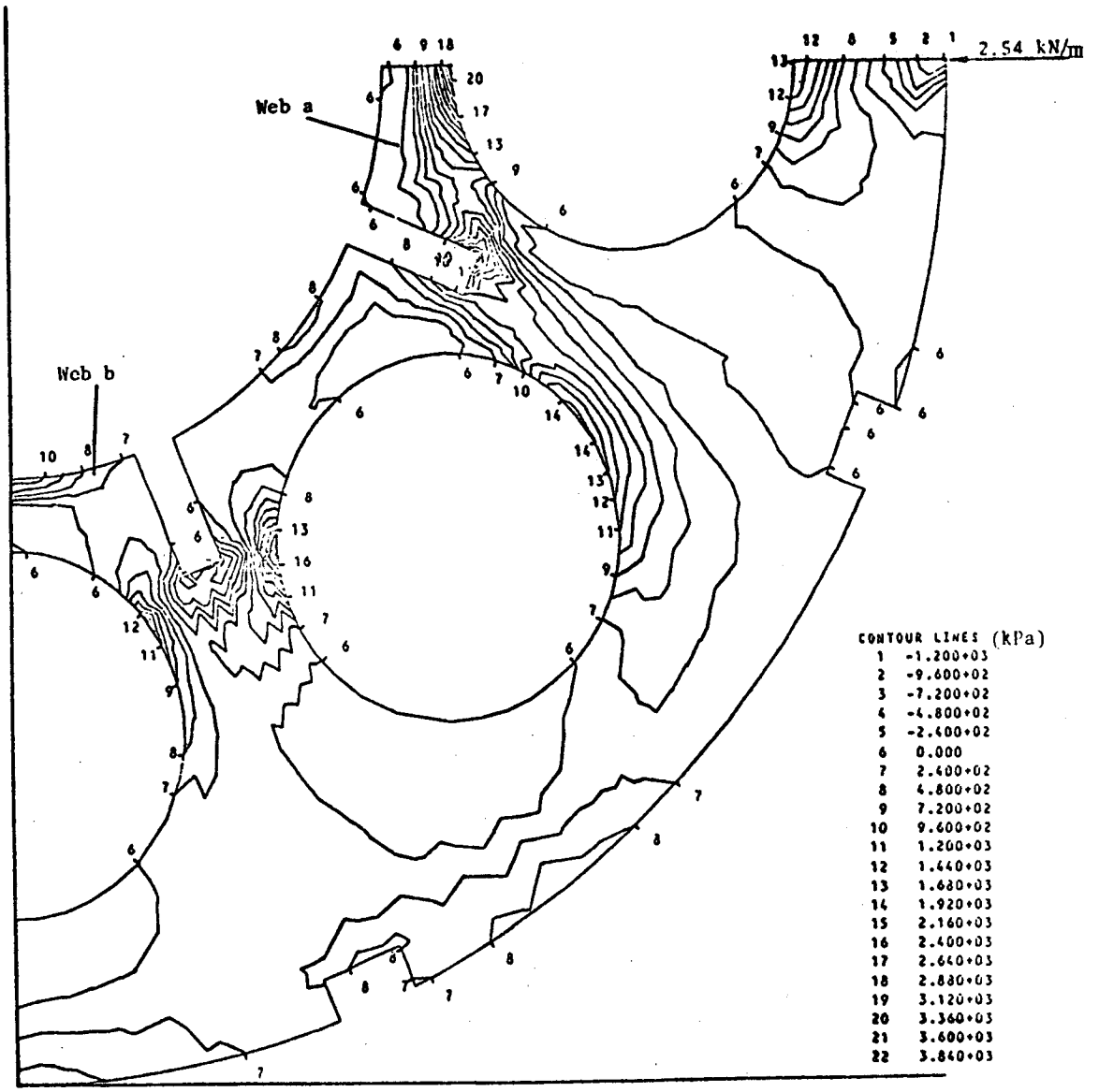

Figure 11 Maximum principal stress in 8-hole specimen under 2.54 kN/m compression load.

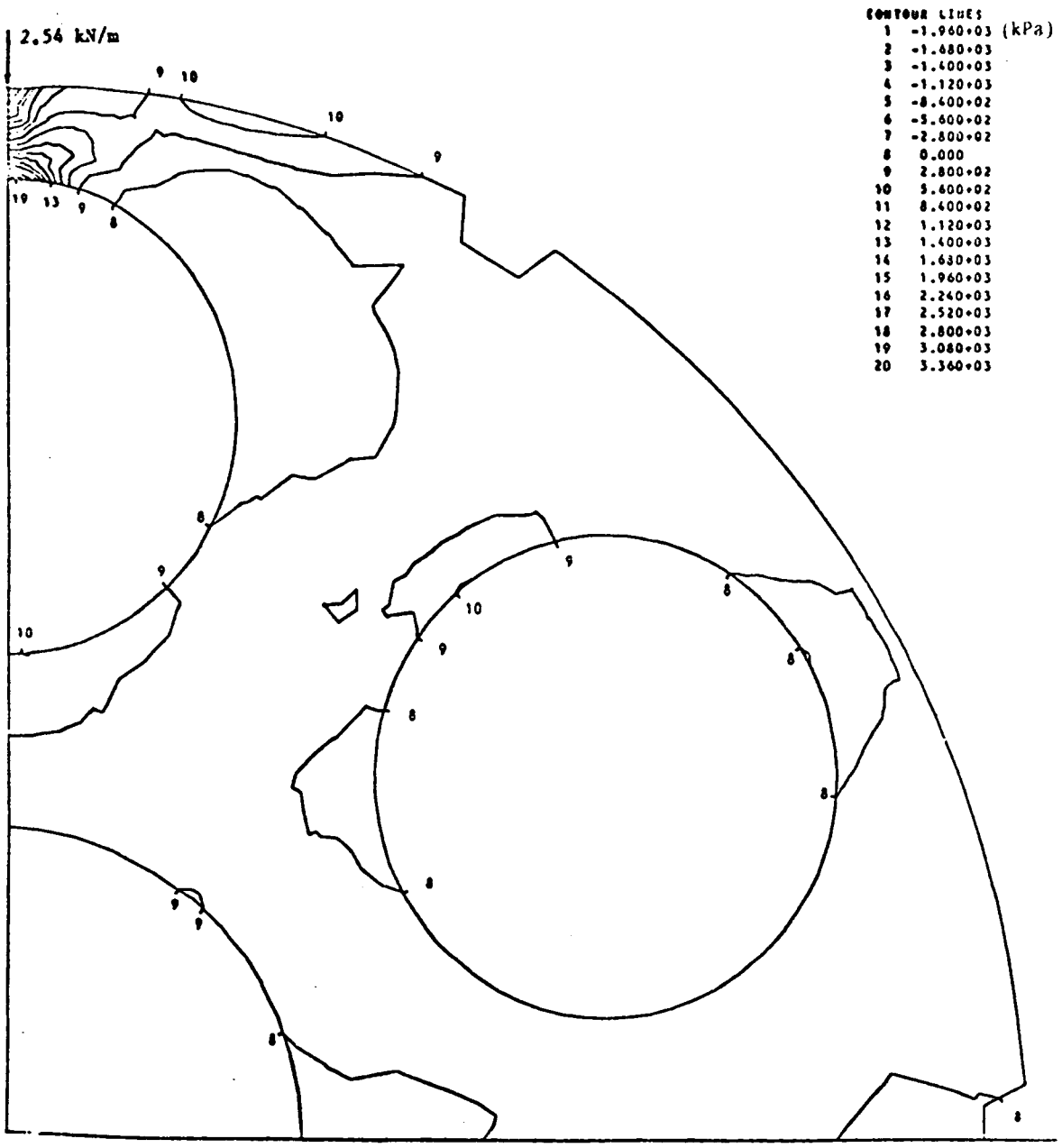

Figure 12 Maximum principal stress in 6-hole specimen under 2.54 kN/m compression load.

of these tests was to measure the strength of irradiated specimens with negligible residual stress to compare with cases where there was substantial residual tension.

The need for tests on unirradiated specimens was also identified. The unirradiated 6- and 8-hole teledial specimens were machined from a graphite log whose strength and elastic modulus in the axial and in-plane directions had been characterized by tensile tests. The tests on the unirradiated specimens serve as controls to the pressure burst and radial compression tests and are used to calibrate failure loads, load-deflection curves, and test methods.

4. ANALYTICAL RESULTS COMPARED WITH EXPERIMENT

The preliminary analytical and experimental results for strip-cutting and ring-cutting tests are compared in Table I. As shown here, the results of ring-cutting experiments[1] agree quite well with the analytical predictions. This indicates that the in-plane stresses are accurately predicted by the analytical methods, at least for elements 3 and 4, whose fast neutron fluence ranged up to 1.9×10^{25} n/m^2. Elements 5 and 6, which were irradiated to higher fluences, have not yet been examined.

For the strips, the analytical and experimental results do not compare so well. The measured bow is at best 40% of that predicted, and the direction of bow is reversed in strips irradiated to higher fluence levels. Possible explanations for this include large errors in the dimensional change data for graphite under irradiation, a large systematic variation in the thermal expansivity of irradiated graphite with irradiation temperature, or mechanically-induced strain imparted when the strips were cut. The variation in thermal expansivity of graphite has been eliminated as a possibility by experiments[1], and the error in irradiation strain data would have to be unreasonably large. The possibility that the bow is caused by the strip-cutting operation is being studied but the initial tests[1] show that the saw has a negligible effect on the unirradiated graphite.

Preliminary measurements of the elongation of strips[1] has cast further doubt on the validity of the strip-cutting technique. The thin strips were found to be about .07% longer after cutting which is about 3 times the predicted elongation due to residual compressive stresses. The thick strips lengthened by a similar amount, even though mean stresses and elongation were predicted to be near zero (slightly positive for 8-hole and slightly negative for 6-hole elements). The elongation of the two strips would imply that they both had a compressive stress of about 14 MPa before cutting. If this were true, there would have to have been a mean axial

TABLE I

COMPARISON OF ANALYTICAL AND EXPERIMENTAL RESULTS
FOR STRIP-CUTTING AND RING-CUTTING EXPERIMENTS

		Change of Diameter After Cutting (mm)		Change of Groove Distance After Cutting (mm)		Bow of Thin Strip (mm)		Bow of Thick Strip (mm)	
Element	Position	Analysis	Experiment	Analysis	Experiment	Analysis	Experiment	Analysis	Experiment
3	5	-.101	-.053	-.299	-.305	--	--	--	--
	15	--	--	--	--	1.61	0.58	2.15	0.84
	25	-.059	-.048	-.195	-.262	--	--	--	--
4	7	-.038	-.056	-.166	-.207	--	--	--	--
	13	--	-.062	--	-.309	2.49	-0.16	2.9	0.67
	23	-.046	-.038	-.176	-.213	--	--	--	--
5	5	--	--	--	--	--	--	--	--
	15	--	--	--	--	1.79	-2.57	2.16	-0.76
	25	--	--	--	--	1.48	0.02	1.85	0.29
6	5	--	--	--	--	1.69	0.20	2.54	0.74
	15	--	--	--	--	2.43	-1.26	2.76	0.37
	25	--	--	--	--	2.26	-0.84	2.62	0.20

tension in the central portion of the 8-hole teledial element of 40 MPa or more to balance the forces. This is unlikely since the axial tensile strength is at most only about 30 MPa. For the 6-hole elements, an even higher tensile stress in the small area removed by the saw (Figure 4) would have been necessary to balance forces.

Preliminary measurements of the peak stress at failure for unirradiated specimens are summarized in Table II. The failure stresses were obtained from Figures 9 through 12 and the measured failure loads[1]. As shown in Table II the stress at failure is always greater than the 8.5 MPa tensile strength of the graphite in the in-plane direction. This result is attributed to the stress gradients at the points of failure which have been found by several investigators (e.g., Brocklehurst and Darby[6]) to increase the failure stress above the uniaxial tensile strength.

Comparison of the preliminary results of pressure burst and radial compression tests on irradiated specimens[1] with similar results on unirradiated specimens has shown a good agreement with predictions. In the case of 6-hole specimens tested under pressure burst and radial compression loads and 8-hole specimens with four inner webs removed tested under radial compression, the failure loads for irradiated specimens were greater than those for unirradiated specimens. This was expected because of the increase in the strength of graphite due to irradiation. For 8-hole specimens under pressure burst and radial compression loads, the failure loads on irradiated specimens were less than those on unirradiated specimens. This was also expected, since the large residual stress peaks in these specimens coincide with the peaks in primary stress. While further analyses and experiments are needed to confirm and quantify these results, the preliminary results are quite encouraging.

TABLE II

FAILURE STRESS IN UNIRRADIATED SPECIMENS

	Failure Stress (MPa)	Stress/Strength
Pressure Burst Tests		
6-Hole	13	1.5
8-Hole	16	1.9
Radial Compression Tests		
6-Hole	36	4.3
8-Hole	19	2.2
8-Hole after Pressure Burst	17	2.0

5. CONCLUSIONS

The principal conclusions at this state of the program are as follows:

1. In-plane stress predictions have been verified by ring-cutting experiments.
2. Axial stress predictions have not been verified by experiment, and the strip-cutting technique is suspected as the cause of the discrepancies.
3. Failure stresses under primary load exceed the uniaxial tensile strength by factors of 1.5 to 4.3 due to stress gradients in the specimens.
4. Radial compression and pressure burst tests on discs cut from teledial elements have successfully demonstrated the effect of residual stresses on strength and have further verified the in-plane stress predictions.

6. REFERENCES

1. Wallroth, C. F., C. M. Miller, J. J. Saurwein, "Residual Stress and Strain Examination in Peach Bottom Fuel Test Elements," paper D5b, 4th International Conference on Structural Mechanics in Reactor Technology, San Francisco, California, August 15-19, 1977.

2. Tzung, F. K., "GTEPC-2D, A Computer Program for Two-Dimensional Graphite Thermal-Elastic-Plastic-Creep Analysis, User's Manual," General Atomic Report GA-A13532, January 31, 1976.

3. Head, J. L., "The Transient Creep of Graphite in a Reactor Environment," paper presented at the Third International Conference on Structural Mechanics in Reactor Technology, London, September 1-5, 1975.

4. Beavan, L. A., "H-327 Graphite - Design Data Package," General Atomic unpublished data, December 1975.

5. Wallroth, C. F., J. F. Holzgraf, and D. D. Jensen, "Post-Irradiation Examination and Evaluation of Peach Bottom Fuel Test Element FTE-6," USERDA Report GA-A13943, General Atomic Company, to be published.

6. Brocklehurst & Darby, Matls. Sci. & Eng., 16, (1974), 91-106.